Acta Crystallographica Section B
Structural Science
ISSN 0108-7681

Structure of *N*-(5-ethyl-[1,3,4]-thiadiazole-2-yl)-toluenesulfonamide by combined X-ray powder diffraction, ^{13}C solid-state NMR and molecular modelling

Adriana Hangan,[a] Gheorghe Borodi,[b] Xenia Filip,[b] Carmen Tripon,[b] Cristian Morari,[b] Luminita Oprean[a] and Claudiu Filip[b]*

[a]University of Medicine and Pharmacy, Department of Inorganic Chemistry, 400010 Cluj, Romania, and [b]National Institute for R&D of Isotopic and Molecular Technologies, 400293 Cluj, Romania

Correspondence e-mail: cfilip@itim-cj.ro

Received 16 March 2010
Accepted 1 October 2010

The crystal structure solution of the title compound is determined from microcrystalline powder using a multi-technique approach that combines X-ray powder diffraction (XRPD) data analysis based on direct-space methods with information from ^{13}C solid-state NMR (SSNMR), and molecular modelling using the GIPAW (gauge including projector augmented-wave) method. The space group is *Pbca* with one molecule in the asymmetric unit. The proposed methodology proves very useful for unambiguously characterizing the supramolecular arrangement adopted by the *N*-(5-ethyl-[1,3,4]-thiadiazole-2-yl)toluenesulfonamide molecules in the crystal, which consists of extended double strands held together by C—H$\cdots\pi$ non-covalent interactions.

1. Introduction

Increasing demands, especially from the pharmaceutical industry, for rapid molecular and crystal structure determination has greatly contributed to expanding the practical applications of X-ray powder diffraction (XRPD), either alone, or in combination with complementary techniques. This is facilitated by the substantial progress made in recent years in the scope and potential of the techniques used in the field (McCusker *et al.*, 1999; Harris *et al.*, 2001; Zhigang *et al.*, 2005). The incorporation of solid-state NMR (SSNMR) parameters, *e.g.* chemical shifts (Harris *et al.*, 2007), torsion angle restraints (Middleton *et al.*, 2002) and inter-molecular distances (Aluas *et al.*, 2009), into the XRPD structure determination process is also regarded as a promising approach, because it has the effect that a correct solution is reached more reliably and in a shorter time. Most of the applications reported so far rely on ^{13}C(^{15}N) cross-polarization magic angle spinning (CP/MAS) NMR spectra, because chemical shifts are sensitive even to small changes in crystal packing and molecular conformation. Such spectra provide information that is useful both before the XRPD search procedure is started, *e.g.* the number of molecules in the asymmetric unit, the presence of more polymorphs in the sample, and information regarding the structural and/or dynamical disorder in the lattice *etc.*, and after the protocol has been completed, for instance to validate the result by comparing the measured chemical shifts with those computed on the obtained crystal structure (Harris *et al.*, 2006; Offerdahl & Munson, 2004; Tam *et al.*, 2003; Tishmack *et al.*, 2003).

In the present work, the latter strategy was successfully applied to determine the crystal structure of *N*-(5-ethyl-[1,3,4]-thiadiazole-2-yl)toluenesulfonamide. The *N*-substituted heterocyclic sulfonamides have found numerous pharmaceutical applications because of their ability to coordinate

biologically important metallic ions. Sulfonamides are also among the ligands commonly used to form complexes with 'nuclease activity'. The aromatic rings in the structure of *N*-substituted sulfonamides can be intercalated between the bases of the DNA chain. This interaction along with the formation of reactive oxygen species (due to the presence of Cu^{2+}) results in the cleavage of the DNA chain (Garcia-Gimenez *et al.*, 2009).

The title compound belongs to a class of ligands of which Cu^{II} complexes are studied for their nuclease activity and also because the [1,3,4]-thiadiazole derivatives (Supuran, 2008) are generally known to have a great *in vivo* stability, and a lack of toxicity for higher vertebrates, including humans. The crystal structure for two of these Cu^{II} complexes was solved in a previous publication (Hangan *et al.*, 2009); however, this was not possible in the case of the free ligands because single crystals of sufficient size and quality could not be grown. Alternatively, a multi-technique approach based on combining complementary information from XRPD, SSNMR and quantum chemical computations in extended (periodic) molecular systems is regarded as an attractive strategy for increasing the reliability of the structure determined from microcrystalline powders (Harris *et al.*, 2007). The results obtained here confirm the usefulness of such an approach, especially with respect to increasing the confidence level in the crystal structure determined from powders, but also to identify the non-covalent interactions responsible for stabilizing the three-dimensional crystal structure of the title compound.

2. Experimental

2.1. Synthesis of the *N*-(5-ethyl-[1,3,4]-thiadiazole-2-yl)toluenesulfonamide ligand

Toluenesulfonylchloride, 2-amino-5-ethyl-[1,3,4]-thiadiazole and pyridine were purchased from commercial sources and used as received. A solution containing 1 mmol of 2-amino-5-ethyl-[1,3,4]-thiadiazole and 0.9 mmol of toluenesulfonylchloride in 6 ml of pyridine was heated at reflux for 1 h, at 333 K. The mixture was added to 10 ml of cold water and stirred for several minutes. The resulting solid was recrystallized from ethanol.

2.2. Physico-chemical characterization

Elemental analysis (C, N, H, S) was performed on a Perkin–Elmer device, using the combustion technique. Fast-ion bombardment (FAB) mass spectra were obtained on a VG Autospec spectrometer in *m*-nitrobenzene solvent. The chemical composition and purity were checked by ^{13}C and ^{1}H NMR – corresponding spectra were recorded on a Bruker Avance 500 spectrometer in DMSO-d_6 solution, and also used to simplify the assignment of the ^{13}C solid-state NMR spectrum. IR spectra were recorded in the 4000–400 cm^{-1} range with a Perkin–Elmer FT-IR 1730 spectrophotometer using powder samples in KBr pellets. The main IR absorption bands were found to be consistent with the structural features of the title compound: 1530 (thiadiazole), 1319 and 1142 $\nu(SO_2)$, 916 $\nu(S-N)$, 678 $\nu(C-S)$, all in cm^{-1}.

2.3. Powder X-ray diffraction and solid-state NMR

X-ray powder diffraction data were recorded with a Bruker D8 Advance powder diffractometer using Cu $K\alpha_1$ radiation (λ = 1.54056 Å). The θ–2θ Bragg–Brentano configuration geometry and incident-beam Ge (111) monochromator were used. The sample was ground to a fine homogeneous powder using an agate pestle and mortar and mounted in a sample holder. The measurements were performed at room temperature within a 2θ range of 3.5–50° in steps of 0.005°.

Solid-state ^{13}C NMR spectra of the *N*-(5-ethyl-[1,3,4]-thiadiazole-2-yl)toluenesulfonamide ligand were recorded at 150.9 MHz ^{13}C Larmor frequency with a Bruker AVANCE III 600 MHz spectrometer operating at room temperature. Standard cross-polarization magic angle-spinning (CP/MAS) experiments were performed at a spinning frequency of n_R = 12 kHz, using a ^{1}H 90° pulse length of 3.2 ms. The ^{13}C NMR spectra were acquired under two-pulse phase-modulated (TPPM) ^{1}H decoupling at 80 kHz by averaging 10 000 scans with a recycle delay of 3 s. The CP transfer was optimized for the first Hartmann–Hahn matching condition ($\nu_{1C} = \nu_{1H} - \nu_R$), where the *rf* fields on the ^{1}H and ^{13}C channels have been calibrated to 52 and 40 kHz, respectively, and the contact pulse was set to 2 ms. The ^{13}C CP/MAS spectrum of *N*-(5-ethyl-[1,3,4]-thiadiazole-2-yl)toluenesulfonamide was calibrated relative to the $^{13}CH_3$ line in TMS (tetramethylsilane) through an indirect procedure which used adamantane as an intermediary standard.

2.4. Computational methods

The isotropic ^{13}C chemical shifts for *N*-(5-ethyl-[1,3,4]-thiadiazole-2-yl)toluenesulfonamide have been computed for molecules in solution and the crystalline phase using the *GAUSSIAN*03 (Frisch *et al.*, 2004) package, and the GIPAW method implemented within the QUANTUM ESPRESSO (QE) suite codes (Giannozzi *et al.*, 2009), respectively. In both cases we started with a geometry optimization of the structure obtained by X-ray powder diffraction, followed by NMR calculations.

For molecules in solution, geometry optimization and NMR calculations were performed at the density functional theory (DFT) level of theory with the OPBE hybrid exchange–correlation functional and the cc-pVTZ basis set. NMR calculations have been performed with the GIAO (gauge including the atomic orbital) method as implemented in *GAUSSIAN*03. The dielectric medium effect was included using the polarizable continuum model (PCM; Miertus *et al.*, 1981) with DMSO as the solvent. In order to express the chemical shifts in p.p.m. we have optimized the geometry of the TMS molecule and then calculated their shielding tensor using the same functional and basis set as in the case of *N*-(5-ethyl-[1,3,4]-thiadiazole-2-yl)toluenesulfonamide.

Table 1
Experimental *versus* computed ^{13}C chemical shifts of *N*-(5-ethyl-[1,3,4]-thiadiazole-2-yl)toluenesulfonamide in the solid state, $\delta^{s}(^{13}C)$ and DMSO-d_6 solution, $\delta^{l}(^{13}C)$, relative to TMS.

The last column shows the difference between the solid- and liquid-state experimental chemical shifts, $\Delta^{sl}_{exp} = \delta^{s}(^{13}C) - \delta^{l}(^{13}C)$.

Site	$\delta^{s}(^{13}C)$ (p.p.m.)			$\delta^{l}(^{13}C)$ (p.p.m.)		
(atom label)	Experimental	Calculated H-relaxed	Calculated all-relaxed	Experimental	Calculated	Δ^{sl}_{exp} (p.p.m.)
C1	14.0	20.2	17.2	12.7	17.6	1.3
C2	23.5	25.6	24.6	24.1	28.5	−0.6
C3	165.7	196.2	180.9	167.9	165.3	−2.2
C4	161.9	177.3	171.1	160.4	156.9	1.5
C5	138.9	151.0	151.3	139.7	134.5	−0.8
C6	127.6	133.6	133.2	130.0	123.3	−2.4
C7	130.5	137.2	139.5	126.2	128.2	4.3
C8	145.0	150.8	156.5	143.1	144.1	1.9
C9	132.0	139.5	143.0	126.2	129.4	5.8
C10	128.3	135.1	134.1	130.0	123.9	−1.7
C11	21.3	22.9	22.0	21.4	23.1	−0.1

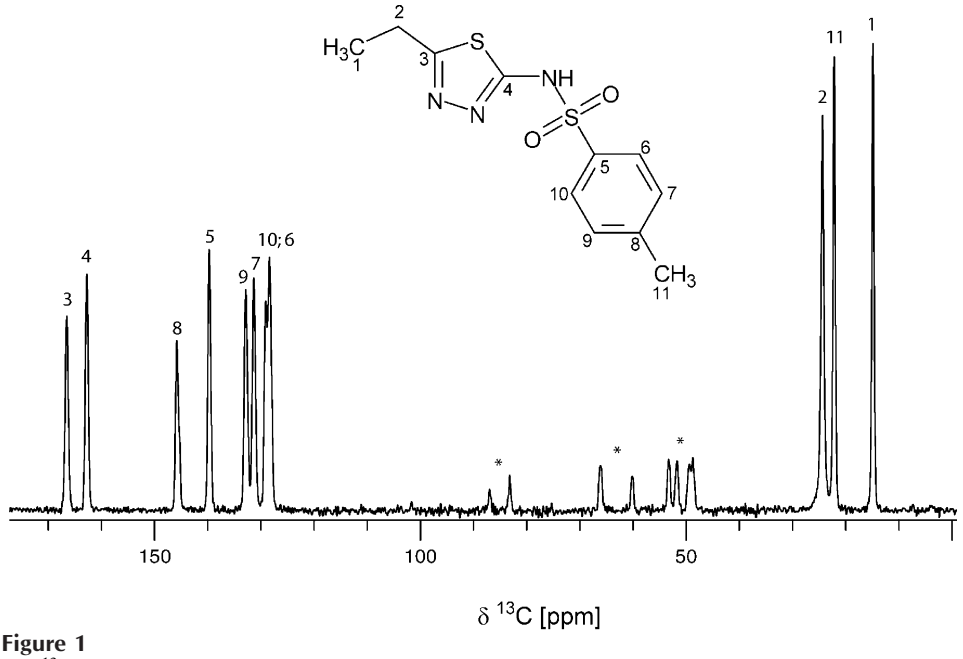

Figure 1
The ^{13}C CP/MAS spectrum of *N*-(5-ethyl-[1,3,4]-thiadiazole-2-yl)toluenesulfonamide. The labelling of the carbons shown in the inset was used for spectral assignment only and should not be confused with the actual labelling incorporated in the name of the title compound. The asterisks indicate spinning sidebands.

For the crystalline phase, the structures obtained by X-ray powder diffraction have been optimized prior to chemical shielding calculations in two different ways:

(i) the positions of the non-H atoms and unit-cell parameters were considered fixed at their diffraction derived values, but the H atoms were allowed to move, and

(ii) by fixing only the unit-cell parameters and allowing the positions of all atoms to be optimized.

QE, which implements density-functional theory using a planewave basis-set, was employed in the first case (H-relaxed) by using the PBE exchange–correlation functional and the Trouiller–Martins norm-conserving pseudopotentials, and a cut-off energy of 40 Ryd. Owing to the size of the system (248 atoms in the unit cell), geometry optimization was performed in the second case (all-relaxed) with the density functional theory code SIESTA (Soler *et al.*, 2002). SIESTA also uses pseudopotentials, but expands the wavefunctions of valence electrons by linear combinations of numerical atomic orbitals. We used a double-zeta polarized (DZP) basis set with an energy cutoff of 25 meV and performed Gamma-point calculations by employing the same generalized gradient approximation (GGA) for the exchange and correlation functional. For the two optimized crystalline structures, the ^{13}C NMR chemical shielding constants were computed in QE with a cut-off energy of 70 Ryd.

3. Results and discussion

3.1. Preliminary information from the ^{13}C CP/MAS spectrum

High-resolution SSNMR spectra for ^{13}C and ^{15}N commonly found in organic solids are intensively used, together with a series of other spectroscopic techniques to solve the structure for a wide range of compounds. The continuous methodological developments and recent technological advances make SSNMR spectroscopy an attractive and accurate tool for elucidating various structural and dynamical features. For example, it is of great importance, especially for pharmaceutical applications, to establish the molecular geometry of a potentially active compound, and to determine whether this compound can exhibit polymorphism or not. SSNMR is widely used for such a purpose, because it is very sensitive in distinguishing between two or more polymorphs of the same crystalline solid (Balimann *et al.*, 1981; Bugay, 2001; Reutzel-Edens & Bush, 2002).

The first step in characterizing a solid form is the assignment of individual resonances to the atoms in the molecule. Depending on the strength of specific solid-state effects (crystal packing, conformational changes, formation of intermolecular hydrogen bonds *etc.*) different assignment methods are used. If these effects are weak, a simple comparison between the solution and solid-state ^{13}C NMR spectra is

Table 2
Representative geometric parameters defining the molecular conformation of *N*-(5-ethyl-[1,3,4]-thiadiazole-2-yl)toluenesulfonamide for the structural models obtained in this work: the XRPD structure solution after the first run, (1), and after the second run, **2**, the DFT geometry optimization of the XRPD model (1) by relaxing all atoms, and the DFT optimized molecular structure in DMSO solution.

	XPRD structure models (1) and **2**	All relaxed (optimized in solid)	DFT (optimized in solution)
Bond lengths (Å)			
C1—C2	(1.530) **1.479**	1.543	1.530
C2—C3	(1.496) **1.555**	1.510	1.493
C3—S1	(1.813) **1.751**	1.779	1.740
C3═N1	(1.350) **1.309**	1.323	1.309
N1—N2	(1.385) **1.373**	1.385	1.350
N2═C4	(1.352) **1.310**	1.330	1.313
S1—C4	(1.818) **1.721**	1.765	1.731
C4—N3	(1.342) **1.400**	1.404	1.384
N3—S2	(1.635) **1.645**	1.725	1.704
S2═O1	(1.437) **1.476**	1.498	1.452
S2═O2	(1.438) **1.439**	1.505	1.452
S2—C5	(1.757) **1.817**	1.791	1.777
C5—C6	(1.404) **1.425**	1.413	1.396
C8—C11	(1.509) **1.525**	1.515	1.500
Bond angles (°)			
C1—C2—C3	(111.2) **110.3**	113.4	114.6
C2—C3—S1	(126.7) **123.6**	122.4	123.2
N1—C3—S1	(107.8) **110.9**	113.8	112.9
C3—S1—C4	(91.8) **87.41**	85.7	86.8
N1—N2—C4	(116.7) **111.0**	112.1	112.5
C4—N3—S2	(124.5) **125.5**	126.6	125.4
N3—S2—C5	(99.49) **99.70**	102.9	106.9
O1—S2—O2	(124.67) **118.8**	121.7	121.4
Dihedral angles (°)			
C1—C2—C3—S1	(−39.6) **−44.37**	−47.3	72.1
S1—C4—N3—S2	(10.6) **13.03**	4.0	51.2
C4—N3—S2—C5	(−133.72) **−133.69**	−128.1	65.6
O1—S2—C5—C6	(30.38) **31.63**	26.8	151.8

sufficient in principle. At the other extreme, notable differences may occur between the two spectra, and full assignment is only possible if more sophisticated ^{13}C–^{13}C two-dimensional correlation techniques (De Paepe *et al.*, 2004) are applied. The ^{13}C CP/MAS spectrum of the title compound is shown in Fig. 1, where the assignment of absorption lines corresponds to the labelling scheme displayed in the inset of Fig. 1. As can be seen from Table 1 there are only small differences between the isotropic chemical shifts measured in solution and the solid state, so that the complete assignment of the ^{13}C resonances could be obtained quite straightforwardly by comparing the two corresponding spectra, and by adequately incorporating the results of molecular modelling (see §3.3). This clearly indicates that crystal packing effects and intermolecular interactions are relatively weak, and no significant conformational changes of the *N*-(5-ethyl-[1,3,4]-thiadiazole-2-yl)toluenesulfonamide molecule are expected in the solid compared with the preferred conformation in solution.

In the ^{13}C CP/MAS spectrum shown in Fig. 1(*b*) the 11 chemically distinct C atoms of the *N*-(5-ethyl-[1,3,4]-thiadiazole-2-yl)-toluenesulfonamide molecule are represented by single resonances, which indicates that the title compound has only one molecule in the asymmetric unit, and also that the sample is not a mixture of different crystalline forms, nor does it contain impurities at detectable concentrations. The information obtained here from a simple inspection of the ^{13}C CP/MAS spectrum is used in the following within the protocol of searching the structure solution from the powder X-ray data.

3.2. Crystal structure solution from the XRPD data

Indexing was performed using the *DICVOL* software (Boultif & Louër, 2004). The best solution corresponds to an orthorhombic unit cell with a = 8.5364, b = 15.0148 and c = 21.3846 Å, and a corresponding volume of V = 2740.914 Å^3. By examining the data with *CHECKCELL* (Laugier & Bochu, 2000) the most probable space group was found to be *Pbca*, which has eight molecules in the unit cell if atoms are set in general positions. From a Le Bail fit of the diffraction pattern we obtained R_p = 0.05, R_{wp} = 0.072. The calculated density considering eight molecules in the unit cell is D_x = 1.37 g cm^{-3}, which represents a reasonable value.

A first starting structural model was obtained by molecular mechanics simulation with *MOLDEN*, where all the bond lengths and bond angles are kept rigid during a search for the structure solution. The structure solution process was carried out using the direct-space search method as implemented in the *DASH* program (David *et al.*, 2006) by adjusting ten degrees of freedom out of which six correspond to the molecular positions and orientations, whereas the remaining four represent the flexible torsion angles of the molecule (see Table 2). The initial model obtained in this way was further used as a starting point for Rietveld refinement with *GSAS* (Larson & Von Dreele, 2000) interfaced by *EXPGUI* (Toby, 2001). A global isotropic temperature factor was refined for all atoms. In order to retain a chemically realistic model several types of soft restraints for bond distances, angles and the planarity of the phenyl ring had to be used. The weight factors (f_d, f_a, f_p) for the distance, angle and planar restraints on the minimization function were gradually reduced in subsequent refinement cycles from 500 to 100. Peak profiles of the reflections in the range 2θ = 3.5–50° were modeled with a pseudo-Voigt peak profile function with 18 terms of which coefficients were parameterized as in Thompson *et al.* (1987) and combined with the asymmetry correction of Finger *et al.* (1994). The background was modeled by a Chebyshev polynomial of the first kind and the U_{iso} values of identical atom types were coupled and a small damping was applied during all refinement stages. Although the structure solution obtained at this stage appears plausible, the quality of the fit with respect to the difference pattern and the magnitude of the corresponding figures-of-merit (R_p = 0.099, R_{wp} = 0.1358, χ^2 = 6.71) could not be considered quite satisfactory, thus calling for further improvements (see §3.4). To do this, the XRPD-obtained crystal structure was employed next as a trial structural model within the ^{13}C NMR chemical shift analysis, which is expected to provide useful clues about particular structural parameters that might not have been refined sufficiently well.

3.3. Experimental *versus* computed ^{13}C NMR chemical shifts

The measured and theoretical ^{13}C NMR chemical shift values, computed on models derived from the XRPD structure solution obtained previously, are compared in Table 1. For this purpose the isotropic shielding constants σ, calculated as described in §2.4, were transformed to chemical shifts relative to TMS using the relationships:

(i) $\delta = \sigma_{TMS} - \sigma$ for the shifts measured in solution, with the TMS shielding constant σ_{TMS} = 189.4 p.p.m. calculated under the same conditions as σ, and

(ii) $\delta = \sigma_{ref} - \sigma$ for those in the solid state, where the reference values σ_{ref} of 165.6 p.p.m. (H-relaxed case) and 163.1 p.p.m. (all-relaxed case) were extracted from the linear fit of the computed shielding constants against experimental shifts, as described in Harris *et al.* (2007).

The mean absolute deviation (MAD) of 3.7 p.p.m. between the experimental and computed $\delta^{l}(^{13}C)$ values in solution falls within typical ranges reported in the literature (Wu *et al.*, 2007) at the level of theory considered in the present work. As can be seen from Table 1, larger contributions to MAD are from the carbon sites closer to the —NH group (C5, C6, C10 and C4), which we attribute to solvent effects that cannot be properly accounted for within the PCM model. Most probably this is because of the strong interaction of the —NH hydrogen with the very polar DMSO oxygen, an assumption which is also confirmed by the large difference between the experimental (∼ 13.9 p.p.m.) and calculated (∼ 7.7 p.p.m.) $\delta^{l}(^{1}H)$ chemical shift for this particular hydrogen site, whereas for all the other H atoms differences of less than 0.5 p.p.m. were obtained. Thus, one can conclude that the DFT optimized molecular conformation of *N*-(5-ethyl-[1,3,4]-thiadiazole-2-yl)toluenesulfonamide in DMSO solution is consistent with the NMR results.

Larger deviations between the experimental and theoretical $\delta^{s}(^{13}C)$ values were obtained in the crystalline phase, with a MAD of 9.1 p.p.m. for the H-relaxed, and 7.6 p.p.m. for the all-relaxed case. Even within these error ranges, the calculated chemical shifts correctly reproduce the relative positioning of the experimental NMR resonances. The observed discrepancies can be partly attributed to the fact that the GIPAW method implemented within the QE suite is less optimized compared with equivalent commercial software (*e.g.* NMR CASTEP; Segal *et al.*, 2002), for which MADs of 2–4 p.p.m. are often reported for molecular systems of similar complexity (Harris *et al.*, 2007; Zheng *et al.*, 2008). Another source of error could be represented by the relatively low value of the cut-off energy we were confined to in the present work: this limitation was imposed by the large number of molecules in the unit cell (eight molecules), which raised the number of distinct atoms that had to be considered within the computations to 248.

The difference between the solid and the liquid state ^{13}C chemical shift values obtained experimentally (Δ^{sl}_{exp} in Table 1) will be discussed in the reminder of this section in terms of particular crystal packing effects. The carbon sites (C4, C5, C6 and C10) that were previously identified as being strongly affected by the interaction with the solvent molecules are however excluded from such an analysis because the interpretation of the observed differences in terms of characteristic structural features could be misleading. The major conclusions derived from the comparison prove to be consistent with the XRPD crystal structure model (and its DFT optimized version). In particular, the smallest Δ^{sl}_{exp} values (< 1 p.p.m.) were obtained for the C atoms (C2 and C11) that are well isolated from the surrounding molecules in the crystalline environment (intermolecular C—H distances > 3 Å), and also show little changes of local structural parameters with respect to the optimized molecular conformation in solution (C2 and C4 co-planar with the thiadiazole and phenyl ring, and only small deviations of the corresponding bond length and angles). A slightly larger Δ^{sl}_{exp} of 1.3 p.p.m. is observed in the case of C1, which is most probably associated with this methyl carbon being in closer contact with an intermolecular —NH proton (C1—

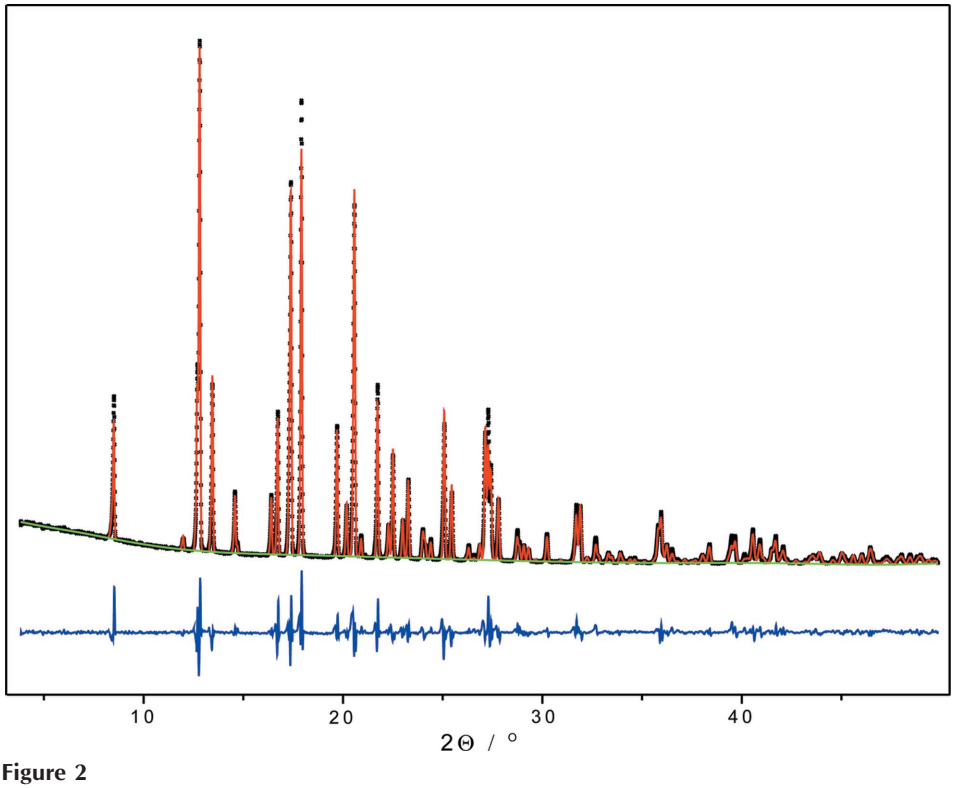

Figure 2
Rietveld plot for *N*-(5-ethyl-[1,3,4]-thiadiazole-2-yl)toluenesulfonamide, where the measured pattern is represented with star symbols, and the calculated pattern with lines, whereas the bottom curve shows the difference pattern.

Table 3
Crystallographic data for *N*-(5-ethyl-[1,3,4]-thiadiazole-2-yl)toluenesulfonamide and refinement summary.

Crystal data	
Chemical formula	$C_{11}H_{13}N_3S_2O_2$
M_r	283.26
Crystal system, space group	Orthorhombic, *Pbca*
a, *b*, *c* (Å)	8.5364 (2), 15.0148 (3), 21.3846 (3)
V (Å^3)	2740.91
Z	8
Radiation type	Cu $K\alpha_1$, λ = 1.5406 Å
Specimen shape, size (mm)	Flat sheet, 1 × 25
Data collection	
Diffractometer	Bruker D8 Advance
Specimen mounting	Bruker sample cup
Data collection mode	Reflection
Scan method	Continuous
2θ values (°)	$2\theta_{min}$ = 3.5, $2\theta_{max}$ = 50, $2\theta_{step}$ = 0.005
Refinement	
R factors and goodness-of-fit	R_p = 0.079, R_{wp} = 0.113, R_{exp} = 0.053, $R(F^2)$ = 0.10350, χ^2 = 4.796
No. of datapoints	9298
No. of parameters	56
No. of restraints	48

H6 $\simeq$ 2.7 Å in the two solid-state models), and also with the difference between the C1—C2—C3—S1 torsion angle obtained for the molecule in solution (72°), and crystalline solid (−40° for the XRPD and −47° for the DFT optimized structure model, respectively).

The largest Δ^{sl}_{exp} deviations correspond to carbon sites (C9 – 5.8 p.p.m., C7 – 4.3 p.p.m.) that are most strongly affected by solid-state effects: in particular, each H4 proton is in close contact with neighboring phenyl π electrons, with an average distance of $\sim$ 2.7 Å between this hydrogen and the phenyl C atoms. This is typical for non-covalent C—H$\cdots\pi$ interactions (Nishio *et al.*, 1998), which can thus be identified as having a decisive contribution in stabilizing the observed three-dimensional crystal structure of the title compound, a conclusion that is also fully supported by the NMR results. According to this model, the *N*-(5-ethyl-[1,3,4]-thiadiazole-2-yl)toluenesulfonamide molecules arrange themselves in the crystal as parallel chain-like superstructures, each of which containing two strands that are held together by C—H$\cdots\pi$ non-covalent interactions (see Fig. 3*b*). Finally, it is also worth mentioning that, compared with the other phenyl C atoms, C9 is more exposed to intermolecular interactions (in addition to C9—H4, this carbon is involved in another short intermolecular contact, C9—H8 of 2.8 Å), which explains for the larger ^{13}C chemical shifts a difference Δ^{sl}_{exp} of 5.8 p.p.m. obtained for this particular site.

3.4. Final crystal structure refinement

Considering the two factors identified above that limit the accuracy of the quantum chemical calculations in QE, more or less equally distributed ^{13}C chemical shift differences over all carbon sites is expected: in practice: however, much larger deviations with respect to the mean value were obtained for the C3 ($\sim$ 30 p.p.m.) and C4 ($\sim$ 15 p.p.m.) C atoms in the H-relaxed case. This result indicates that significant contributions might also be related here with characteristic structural features of the thiadiazole ring, a conclusion supported by the following facts:

(i) These differences could be significantly reduced ($\sim$ 15 p.p.m. for C3, and $\sim$ 9 p.p.m. for C4) for the structure obtained after relaxing the positions of all atoms.

(ii) Geometrical parameters (bond lengths and angles) related to these particular carbon sites in the all-relaxed case are closer to the values obtained for the molecule in solution than the corresponding parameters in the XRPD structural model (see the data listed in Table 2), which is to be expected given the small difference between the solution and solid-state C3 and C4 chemical shifts.

Thus, an improved molecular geometry in the crystal could be obtained in principle by combining experimental NMR chemical shifts with molecular modeling. In particular, the structural model determined in the all-relaxed case appears to better approach the real molecular conformation in the crystal of the title compound: therefore, this was employed next as a starting structural model in a second run of the XRPD structure determination process. However, except for choosing a different initial (rigid – with respect to the bond lengths and angles) structural fragment, the structure solution and the Rietveld structure refinement stages were performed

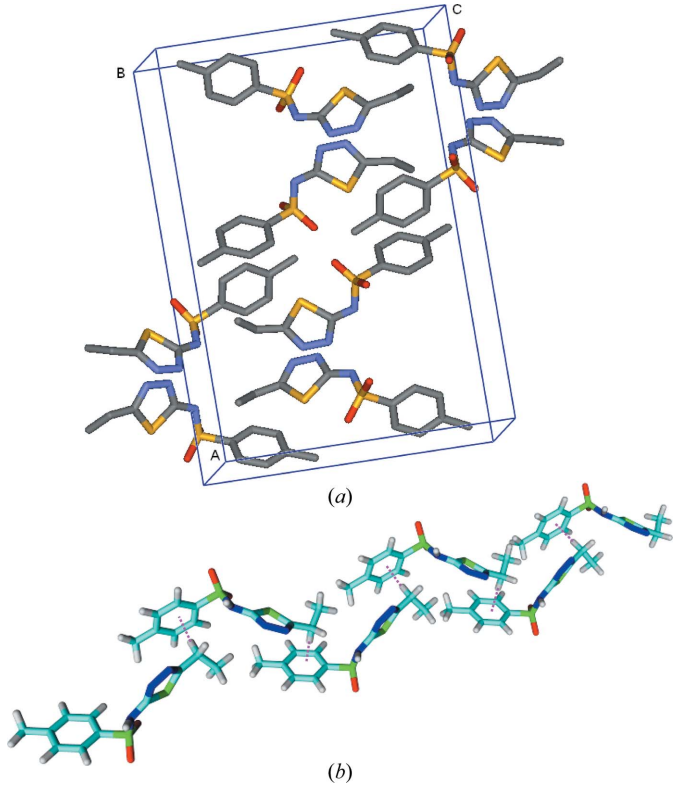

Figure 3
(*a*) Crystal packing of the eight *N*-(5-ethyl-[1,3,4]-thiadiazole-2-yl)toluenesulfonamide molecules in the unit cell of the title compound, as determined from the analysis of XRPD data; (*b*) supramolecular arrangement of the *N*-(5-ethyl-[1,3,4]-thiadiazole-2-yl)toluenesulfonamide molecules in crystals in the form of double strands coupled by C—H$\cdots\pi$ non-covalent interactions (emphasized through dotted lines).

by following exactly the same steps as described in §3.2, so that here we only present the final results. The observed, calculated and difference patterns after Rietveld refinement are shown in Fig. 2, and the crystal packing of the eight *N*-(5-ethyl-[1,3,4]-thiadiazole-2-yl)toluenesulfonamide molecules in the unit cell is displayed in Fig. 3(*a*). Also, details of the structural parameters and refinement are given in Table 3.[1] As a most prominent result one should mention here that using a more realistic starting model had the effect that a better fit of the X-ray diffraction pattern could be obtained (R_p = 0.079, R_{wp} = 0.113, χ^2 = 4.78) at the end of the Rietveld refinement stage.

4. Conclusions

The crystal structure of *N*-(5-ethyl-[1,3,4]-thiadiazole-2-yl)toluenesulfonamide, that belongs to a class of ligands of which Cu^{II} complexes show important nuclease activity, has been determined from microcrystalline powder. Information about the number of molecules in the asymmetric unit and sample quality have been extracted from the ^{13}C CP/MAS spectrum and used to analyse the X-ray powder diffraction pattern. First, a crystal structure with an R_p value of 0.099 was determined by a direct-space method using the simulated annealing algorithm, and followed by Rietveld refinement. The addition of H atoms and geometry optimization were performed starting from the XRPD structural model for the molecule in crystal and DMSO solution. On the optimized structures, DFT computations of ^{13}C chemical shifts were run by employing the GIPAW and GIAO methods. Within the error ranges characteristic of the programs implementing these two methods, analysis indicated a geometrically optimized model that better reproduces the experimental $\delta(^{13}C)$ data. A second run of the XRPD crystal structure determination was then performed using this model as a starting structure, which resulted in an improved quality of the fit between the experimental and calculated powder patterns, hence an increased confidence level in the determined crystal structure. Finally, the comparison between the solution and solid-state ^{13}C chemical shift values enabled conclusions to be drawn with respect to particular crystal packing effects, as well as to the interactions responsible for stabilizing the three-dimensional crystal structure of the title compound.

Financial support from ANCS (project 61–003) and CNCSIS (project IDEI 872) is gratefully acknowledged. We also thank Dr Adrian Parnau for useful discussions.

References

Aluas, M., Tripon, C., Griffin, J. M., Filip, X., Ladizhansky, V., Griffin, R. G., Brown, S. P. & Filip, C. (2009). *J. Magn. Reson.* **199**, 173–187.
Balimann, G. E., Groombridge, C. J., Harris, R. K., Packer, K. J., Say, B. J. & Tanner, S. F. (1981). *Philos. Trans. R. Soc. London Ser. A*, **299**, 643–663.
Boultif, A. & Louër, D. (2004). *J. Appl. Cryst.* **37**, 724–731.
Bugay, D. E. (2001). *Adv. Drug Deliv. Rev.* **48**, 43–65.
David, W. I. F., Shankland, K., van de Streek, J., Pidcock, E., Motherwell, W. D. S. & Cole, J. C. (2006). *J. Appl. Cryst.* **39**, 910–915.
De Paepe, G., Lesage, A., Steuernagel, S. & Emsley, L. (2004). *Chem. Phys. Chem.* **5**, 869–875.
Finger, L. W., Cox, D. E. & Jephcoat, A. P. (1994). *J. Appl. Cryst.* **27**, 892–900.
Frisch, M. J. *et al.* (2004). *GAUSSIAN*03, Revision C.02. Gaussian, Inc., Wallingford, CT, USA.
Garcia-Gimenez, J. L., Alzuet, G., Gonzalez-Alvarez, M., Liu-Gonzalez, M., Castineiras, A. & Borras, J. (2009). *J. Inorg. Biochem.* **103**, 243–255.
Giannozzi, P. *et al.* (2009). *J. Phys. Condens. Matter*, **21**, 395502.
Hangan, A., Borras, J., Liu-Gonzalez, M. & Oprean, L. (2009). *Rev. Chim.* **8**, 755–759.
Harris, K. D. M., Tremayne, M. & Kariuki, B. M. (2001). *Angew. Chem. Int. Ed.* **40**, 1626–1651.
Harris, R. K., Hodgkinson, P., Pickard, C. J., Yates, J. R. & Zorin, V. (2007). *Magn. Reson. Chem.* **45**, S174–S186.
Harris, R. K., Joyce, S., Pickard, C. J., Cadars, S. & Emsley, L. (2006). *Phys. Chem. Chem. Phys.* **8**, 137–143.
Larson, A. C. & Von Dreele, R. B. (2000). LAUR. Los Alamos National Laboratory Report. Los Alamos, New Mexico, USA.
Laugier, J. & Bochu, B. (2000). *CHECKCELL*, Collaborative Computational Project Number 14 (CCP14). Laboratoire des Materiaux et du Génie Physique de l'Ecole Supérieure de Physique de Grenoble, France.
Middleton, D. A., Peng, X., Saunders, D., Shankland, K., David, W. I. F. & Markvardsen, A. J. (2002). *Chem. Commun.* **17**, 1976–1977.
Miertus, S., Scrocco, E. & Tomasi, J. (1981). *Chem. Phys.* **55**, 117–129.
McCusker, L. B., Von Dreele, R. B., Cox, D. E., Louër, D. & Scardi, P. (1999). *J. Appl. Cryst.* **32**, 36–50.
Nishio, M., Hirota, M. & Umezawa, Y. (1998). *The CH/π Interaction, Evidence, Nature and Consequences.* New York: Wiley-VCH.
Offerdahl, T. J. & Munson, E. J. (2004). *Am. Pharm. Rev.* **7**, 109.
Reutzel-Edens, S. M. & Bush, J. K. (2002). *Am. Pharm. Rev.* **5**, 112.
Segal, M. D., Lindan, P. J. D., Probert, M. J., Pickard, C. J., Hasnip, P. J., Clark, S. J. & Payne, M. C. (2002). *J. Phys. Condens. Matter*, **14**, 2717–2744.
Soler, J. M., Artacho, E., Gale, J. D., Garcia, A., Junquera, J., Ordejon, P. & Sanchez-Portal, D. (2002). *J. Phys. Condens. Matter*, **14**, 2745–2780.
Supuran, C. T. (2008). *Nat. Rev. Drug Discov.* **7**, 168–181.
Tam, C. N., Cowan, J. A., Schultz, A. J., Young, V. G. Jr, Trouw, F. R. & Sykes, A. G. (2003). *J. Phys. Chem. B*, **107**, 7601–7606.
Tishmack, P. A., Bugay, D. E. & Bryn, S. R. (2003). *J. Pharm. Sci.* **92**, 441–474.
Thompson, P., Cox, D. E. & Hastings, J. B. (1987). *J. Appl. Cryst.* **20**, 79–83.
Toby, B. H. (2001). *J. Appl. Cryst.* **34**, 210–213.
Zheng, A., Liu, S. B. & Deng, F. (2008). *J. Comput. Chem.* **30**, 222–235.
Zhigang, P., Cheung, E. Y., Harris, K. D. M., Constable, E. C. & Housecroft, C. E. (2005). *Cryst. Growth Des.* **5**, 2084–2090.
Wu, A., Zhang, Y., Xu, X. & Yan, Y. (2007). *J. Comput. Chem.* **28**, 2431–2442.

[1] Supplementary data for this paper are available from the IUCr electronic archives (Reference: ZB5014). Services for accessing these data are described at the back of the journal.